UDC 536.42:669.297

Yahya Al-Khatatbeh[1,*], Khaldoun Tarawneh[1], Hussein Al-Taani[2], Kanani K. M. Lee[3]

[1]Department of Basic Sciences, Princess Sumaya University for Technology, Amman, Jordan

[2]School of Basic Sciences and Humanities, German Jordanian University, Amman, Jordan

[3]Department of Geology and Geophysics, Yale University, New Haven, Connecticut, USA

**y.alkhatatbeh@psut.edu.jo*

Theoretical and experimental evidence for a post-cotunnite phase transition in hafnia at high pressures

Using first-principles density-functional theory (DFT) computations, we have predicted a new post-cotunnite (OII) phase of hafnia (HfO_2) at high pressures. Our computations, using the generalized gradient approximation (GGA), predict a phase transition from OII to a Fe_2P-type structure at ~ 120 GPa (~ 140 GPa) with a slight volume collapse at the transition pressure of ~ 0.2 % (~ 0.1 %) between the two phases using the second- (third-) order Birch-Murnaghan equation of state, respectively. The prediction of the new phase is consistent with recent experiments and computations performed on similar dioxides titania (TiO_2) and zirconia (ZrO_2) at extreme pressure-temperature conditions. Importantly, our theoretical prediction for the OII $\rightarrow$ Fe_2P transition in HfO_2 is experimentally supported by the re-analysis of X-ray diffraction patterns of HfO_2 at extreme pressure-temperature (p, T) conditions. Additionally, the equation of state and hardness of the predicted phase have been computed and show that Fe_2P-type phase while less compressible than the OII phase is nearly identical in hardness, indicating that none of the HfO_2 phases qualify as superhard.

Keywords*: phase transitions, equation of state, hardness, first-principles, x-ray diffraction, phase stability.*

INTRODUCTION

Hafnia (HfO_2) is characterized by its structural stability as well as its dielectric properties as a high-*k* dielectric material. Therefore, HfO_2 has important industrial applications in optical coatings [1, 2] and as a gate insulator in advanced metal-oxide-semiconductor technology [3–5], and it has attracted interest as a suggested candidate for resistive-switching memories [6–8]. As a result, HfO_2 has received a great deal of attention during the last few decades to study its various mechanical properties, and one of the ongoing interests is investigating its high-pressure/temperature behavior. Thus, many experimental [9–20] and theoretical [9, 21–25] studies have investigated the high-pressure, high-temperature behavior of HfO_2. The *first-principles* computations [9, 22, 25] predict that HfO_2 undergoes the following sequence in crystal structure on compression: baddeleyite $\rightarrow$ OI $\rightarrow$ OII in good agreement with measurements [9, 11, 26].

It should be noted that the high-pressure behavior of HfO_2 is very similar to that of zirconia (ZrO_2) [9, 11, 22, 25–31] as both dioxides undergo the same high-pressure phase transition sequence, and the equation of state (EOS) and the mechanical hardness of their various phases are comparable. Additionally, this similarity extends to titania (TiO_2) where experiments and calculations have shown that the three dioxides overlap the same sequence: baddeleyite → OI → OII with comparable mechanical properties [24, 32–38].

Until recently, the cotunnite (OII) phase (Fig. 1) of the three transition metal dioxides (TMDs) has been thought to be the highest-pressure and densest phase among these dioxide phases. However, recent high-pressure diamond-anvil cell (DAC) experiments and density-functional theory (DFT) computations have shown that Fe_2P-type structure phase (see Fig. 1) is denser and more stable than OII for TiO_2 [39] and ZrO_2 [40] at high pressures. For example, experimentally, Fe_2P phase becomes stable at (210 GPa, 4000 K) [39] and (175 GPa, 3000 K) [40] for TiO_2 and ZrO_2, respectively. Theoretically, the generalized gradient approximation (GGA) computations predict the OII → Fe_2P transition to occur at 161 GPa (for TiO_2) [39] and at 143 GPa (for ZrO_2) [40]. For HfO_2, the most extreme conditions that have been achieved thus far is 105 GPa and 1800 K [9], and in spite of these conditions, the OII phase was concluded to be the highest-pressure phase of HfO_2, with no claim of transition to a new phase (Fe_2P) in that study [9]. Additionally, the Fe_2P structure has been predicted for $Ti(Zr/Hf)_2O_6$ photocatalysts using *first-principles* computations [41].

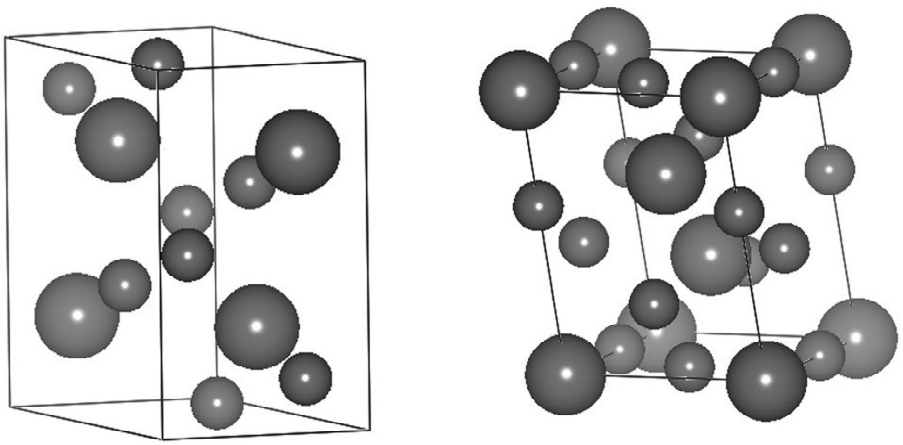

Fig. 1. Crystal structures and summary of the structural properties of HfO_2 phases [62]. The larger spheres represent the Hf atom, while the smaller spheres represent the O atom. The OII phase has been observed in TiO_2, ZrO_2, and HfO_2 [9, 11, 27–29, 32, 34, 35, 63] while Fe_2P phase has been previously observed in TiO_2 [39] and ZrO_2 [40].

While other structures can be theoretically tested at high pressure for HfO_2, our focus is on Fe_2P-type structure as it has been already experimentally observed for similar dioxides. Consequently, and due to the similarity in the three TMDs, we test the stability at high pressures and the EOS of Fe_2P–HfO_2 phase for the first time using DFT computations as well as a re-examination of previous measurements for the presence of this phase. However, we should note that although Fe_2P is not unexpected for HfO_2, to our knowledge it has not been experimentally or theoretically confirmed yet.

In general, the synthesis of new high-pressure phases is an important route to produce new materials with enhanced properties, and the synthesis conditions play a very important role due to the difficulties in producing ultrahigh p, T-conditions. Therefore, reducing the extreme p, T-synthesis conditions could be possible in case of synthesizing the same high-p phase for a different material that greatly overlaps in the behavior and properties with a material that requires much more extreme conditions. As a result, we examine the possibility of synthesizing Fe_2P–HfO_2 at noticeably lower p, T-conditions compared to similar TMDs TiO_2 and ZrO_2.

THEORETICAL METHODS

To study the phase stability and the EOSs of HfO_2, we used static *first-principles* computations performed within the framework of DFT [42]. The projector-augmented wave (PAW) formalism [43, 44] was used to treat the interactions between the atoms having a core radii of 2.600 bohr for hafnium (Hf) and 1.520 bohr for oxygen (O) with the valence configuration of $5p^6 6s^2 5d^2$ for Hf and $2s^2 2p^4$ for O. Following previous high-pressure computations performed on HfO_2 [9, 22, 25], the electronic exchange and correlation effects were treated within the GGA [45]. We performed our calculations using the VASP software package [46–49] with an energy cutoff of 600 eV and Γ-centered k-point meshes [50]. Our computations yielded sufficient convergence to better than ~ 0.1 meV/atom in the total energies for both phases and pressures were converged to better than 0.1 GPa. The Brillouin zone integration was performed using the following k-point meshes for the HfO_2 phases: 4×8×4 for OII and 6×6×10 for Fe_2P. Scalar-relativistic effects are taken into account in the PAW potentials [43, 51]. For a fixed volume, all internal degrees of freedom and unit-cell parameters of the structure were optimized simultaneously during the geometry optimizations. The ground-state energy for each phase was determined for 15–16 volumes, which encompass the (expected) experimental range for each phase. The investigated HfO_2 phases remain insulators up to the highest pressures achieved in this study. The EOS parameters for each phase were obtained by fitting the total energy as a function of volume to a second-(third-) order Birch-Murnaghan equation of state (BM-EOS) [52] (Table 1). The calculated mechanical hardness for each phase was obtained using a scaling model that has been proposed to estimate the hardness in ionic and covalent materials [53].

RESULTS AND DISCUSSION

Compressibility and equation of state

The calculated EOS parameters for the OII and Fe_2P phases of HfO_2 as well as reported values from previous work on similar TMDs TiO_2 [39] and ZrO_2 [40] are summarized in Table 1. The calculated bulk modulus we have obtained for Fe_2P–HfO_2 using the second-order BM-EOS [52] is 288 (2) GPa, which is ~ 6.3 % higher than our calculated K_0 of OII–HfO_2. Therefore, Fe_2P is the most incompressible phase of HfO_2 proposed thus far, consistent with its TiO_2 and ZrO_2 counterparts.

To our best knowledge, the Fe_2P phase has not been tested previously for HfO_2 and, thus, there are no available experimental or theoretical data on Fe_2P–HfO_2 to compare with. However, this phase has been tested using both experiment and theory for the other two TMDs TiO_2 [39] and ZrO_2 [40], and it has been shown that Fe_2P becomes more stable than OII at high pressures. Because of this similarity, we

compare the trends in EOS of OII–HfO_2 versus Fe_2P–HfO_2 with their corresponding EOSs of TiO_2 [39] and ZrO_2 [40].

Table 1. Theoretical EOSs of OII and Fe_2P phases of TiO_2, ZrO_2, and HfO_2 and the calculated and measured transition pressure between the two phases for each dioxide. Our EOS is determined from GGA computations using the second- (third-) order BM-EOS [52]. For comparison, we list other theoretical and experimental results [39, 40]. 1σ uncertainties are given in parentheses

Dioxide	Phase	Equation of state			OII → Fe_2P transition pressure		Reference
		V_0, Å^3	K_0, GPa	K_0'	experiment	theory (GGA)	
TiO_2	OII	26.20	239.9	4.2	210 GPa and 4000 K	161 GPa	[39]
	Fe_2P	26.70	272.1	4			
ZrO_2	OII	30.66	258	4 (fixed)	175 GPa and 3000 K	143 GPa	[40]
		30.78	242	4.24			
	Fe_2P	30.34	272	4 (fixed)			
		30.43	260	4.18			
HfO_2	OII	30.06 (0.06)	271 (3)	4 (fixed)	Close to 105 GPa and 1800 K*	120 GPa (using second-order BM-EOS) and 140 GPa (using third-order BM-EOS)	This work
		30.25 (0.05)	239 (5)	4.52 (0.09)			
	Fe_2P	29.69 (0.03)	288 (2)	4 (fixed)			
		29.74 (0.01)	270 (1)	4.32 (0.02)			

*See Results and Discussion.

It is important to note that we compare our calculated K_0 of Fe_2P–HfO_2 with previous computations rather than measurements in order to ensure a fair comparison, and although experiments have confirmed the stability of the Fe_2P phase for both TiO_2 [39] and ZrO_2 [40], the EOS of Fe_2P–HfO_2 has not been measured. Our comparison (see Table 1), using our second-order BM-EOS parameters, shows that the increase in K_0 between OII and Fe_2P is ~ 9.2 % and ~5.4 % for TiO_2 [39] and ZrO_2 [40], respectively, which is in good agreement with our calculations (~ 6.3 %) for HfO_2.

Additionally, to better understand the compressional behavior of the newly predicted Fe_2P–HfO_2 in comparison to the experimentally confirmed Fe_2P–ZrO_2 [40], in Fig. 2 we show the change in the normalized unit-cell parameters (a/a_0 and c/c_0) for Fe_2P–HfO_2 as a function of pressure as determined by GGA calculations. Our computations suggest anisotropic compression in the Fe_2P-type crystal structure for HfO_2 as the unit-cell parameter c is noticeably more compressible (linear modulus K_{0c} = 209 (5) GPa) than parameter a (linear modulus K_{0a} = 340 (3) GPa) when fit to a Birch-Murnaghan-like fit to the respective lattice parameters [54] which nicely agrees with Fe_2P–ZrO_2 measurements (Table 2) [40].

Phase stability

We have tested the relative stability of the two phases in this study and find the transition from OII to Fe_2P occurs at ~ 120 GPa (~ 140 GPa) using the second- (third-) order BM-EOS [52] (Fig. 3), suggesting that Fe_2P is the highest-pressure phase among known HfO_2 polymorphs. This prediction agrees well with previous

measurements and computations performed on similar dioxides TiO_2 [39] and ZrO_2 [40] that have confirmed the OII Fe_2P transition at ultrahigh pressures experimentally. Specifically, using high-resolution synchrotron powder X-ray diffraction (XRD), high-pressure laser-heated DAC experiments have confirmed the OII $\rightarrow$ Fe_2P transition under extreme conditions of pressure and temperature, where Fe_2P has been observed at (210 GPa, 4000 K) [39] and (175 GPa, 3000 K) [40] for TiO_2 and ZrO_2, respectively. Furthermore, static DFT computations using GGA have predicted this transition to occur at 161 GPa [39] and 143 GPa [40] for TiO_2 and ZrO_2, respectively. Thus, the trend in the transition pressure to the Fe_2P phase supports our findings that the OII $\rightarrow$ Fe_2P transition in HfO_2 is likely to occur at lower pressures than it does for TiO_2 or ZrO_2.

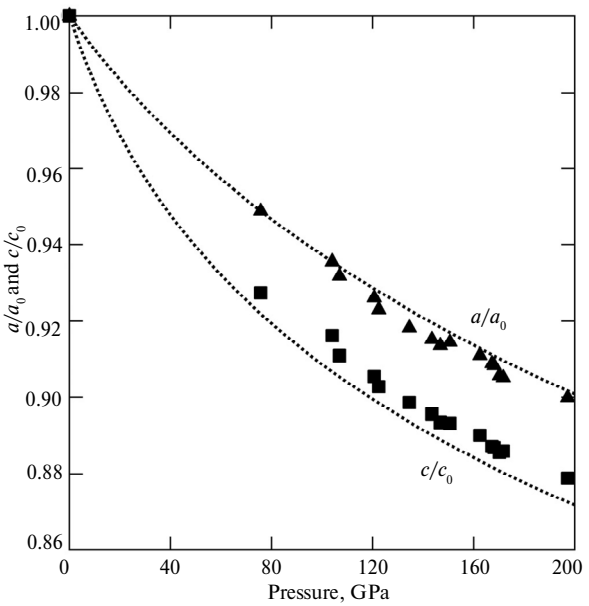

Fig. 2. The change in the normalized unit-cell parameters (a/a_0 and c/c_0) for Fe_2P–HfO_2 as a function of pressure as determined by GGA calculations. Dotted lines indicate the third-order linear BM-EOS [52] for a/a_0 (upper curves) and c/c_0 (lower curves) axes (see Table 2). Our calculations are in excellent agreement with recent measurements [40] on TMD Fe_2P–ZrO_2 (a/a_0: solid triangles and c/c_0: solid squares). The unit-cell parameter c is predicted to be more compressible than parameter a as pressure increases in excellent agreement with recent measurements [40] on Fe_2P–ZrO_2.

Table 2. Calculated linear second- (third-) order BM-EOSs for the unit-cell parameters (a and c) of Fe_2P–HfO_2. 1σ uncertainties are given in parentheses

Equation of State	Linear EOS of unit-cell parameter a			Linear EOS of unit-cell parameter c		
	a_0, Å	K_{0a}, GPa	K_{0a}'	c_0, Å	K_{0c}, GPa	K_{0c}'
Second-order BM	5.602 (0.002)	340 (3)	4 (fixed)	3.280 (0.005)	209 (5)	4 (fixed)
Third-order BM	5.598 (0.002)	360 (5)	3.69 (0.07)	3.286 (0.002)	163 (4)	5.29 (0.11)

Additionally, experimentally, the most extreme p, T-conditions that have been achieved on HfO_2 thus far is 105 (10) GPa and heated up to ~ 1800 K, where OII

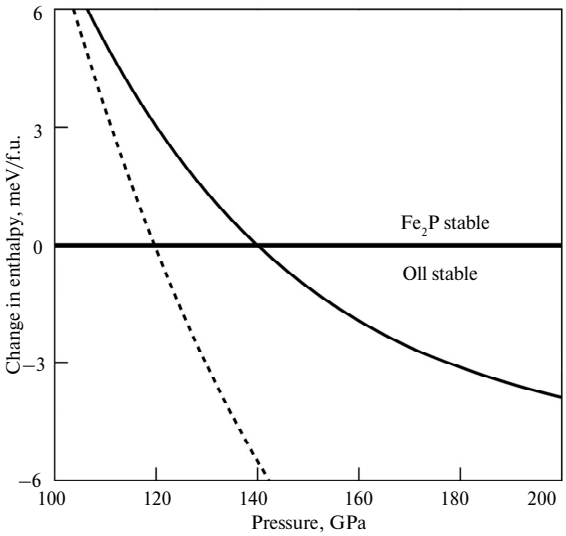

Fig. 3. Change in enthalpy with respect to OII phase versus pressure of one HfO_2 formula unit as determined by GGA calculations. The transition pressure from OII to Fe_2P is ~ 120 GPa and ~140 GPa using a second- (dashed curve) and third- (solid curve) order BM-EOS [52], respectively.

was claimed to be the only phase observed at these conditions [9]. However, considering the *p*, *T*-trend discussed above as well as the effects of thermal pressure [55–57], we infer that the *p*, *T*-conditions achieved in this study [9] are likely close for the predicted phase transformation OII → Fe_2P. Therefore, we have reviewed the room-temperature, post-heated at 1800 K XRD pattern of HfO_2 (Fig. 4) at 105 GPa from that study [9], and have noticed that there are three very weak unexplained XRD peaks in which one of them appears as a left shoulder to the most intense peak of OII phase (OII: 102 reflection). Consequently, our analysis has confirmed that the unexplained peaks may belong to Fe_2P phase (201 and 101 reflections) and the shoulder-like peak is likely to belong to Fe_2P phase (110 reflection). Additionally, these three peaks (201, 101 and 110) correspond to the most intense peaks observed in that phase [39, 40], and, therefore, are expected to be the first peaks to be observed in an emerging Fe_2P-structured HfO_2. Moreover, the measured *d*-spacing values that correspond to the three peaks yield small residuals (≤ ±0.0085 Å) from the expected values given the resultant unit-cell parameters (Table 3). Additionally, the measured unit-cell parameters and volume calculated from these reflections nicely agrees with our computations at 105 GPa (Fig. 5, Table 3). This analysis provides us with an important indication for the occurrence of the OII → Fe_2P transition in HfO_2 and additional experimental evidence that supports our computations for OII → Fe_2P transition at *p*, *T*-conditions greater than (but near to) 105 GPa and 1800 K.

We note that the OII → Fe_2P transition in HfO_2 is a first-order transition associated with a slight volume change (see below) and a small change in enthalpy. The change in enthalpy with respect to pressure ($\Delta H/\Delta P$) for this transition is ~ $3.27\cdot10^{-4}$ eV·GPa^{-1} (~ –0.032 kJ·mol^{-1}·GPa^{-1}) and ~ $1.22\cdot10^{-4}$ eV·GPa^{-1} (~ –0.012 kJ·mol^{-1}.GPa^{-1}) using the second- (third-) order BM-EOS [52], respectively (see Fig. 3). This is similar to the value obtained for ZrO_2 (~ –0.016 kJ·mol^{-1}·GPa^{-1}) [40] and the value obtained for TiO_2 (~ –0.032 kJ·mol^{-1} GPa^{-1}) [39]. Consequently, this may indicate a sluggish transition across the OII → Fe_2P transition in HfO_2 due to

kinetics which is evidenced by the experimentally observed coexistence of the two phases at high p, T-conditions (see Fig. 4).

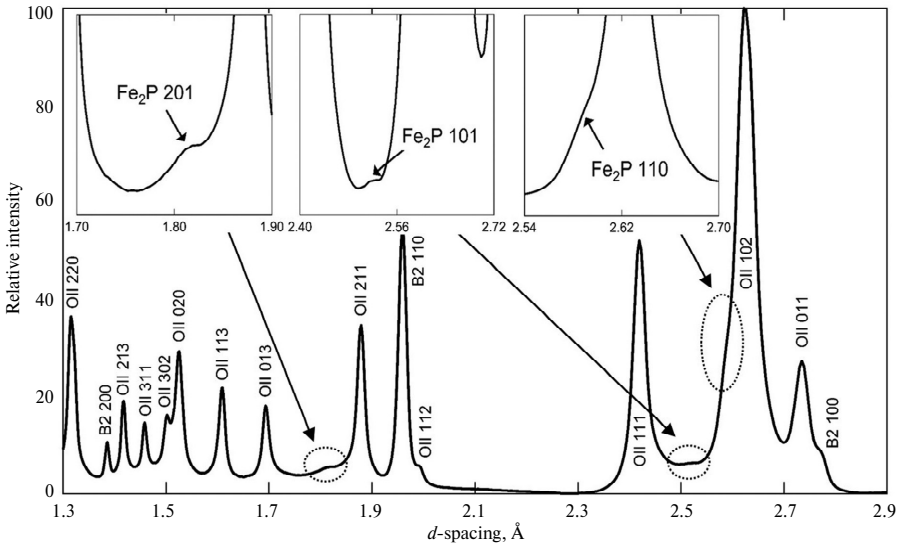

Fig. 4. XRD pattern of HfO_2 at ~ 105 GPa after heating to ~ 1800 K [9]. Fe_2P–HfO_2, OII–HfO_2, and NaCl B2 Miller indices are shown for respective XRD reflections. Insets show zoomed-in regions that are shown in dashed ellipses of the three observed weak XRD reflections of Fe_2P phase.

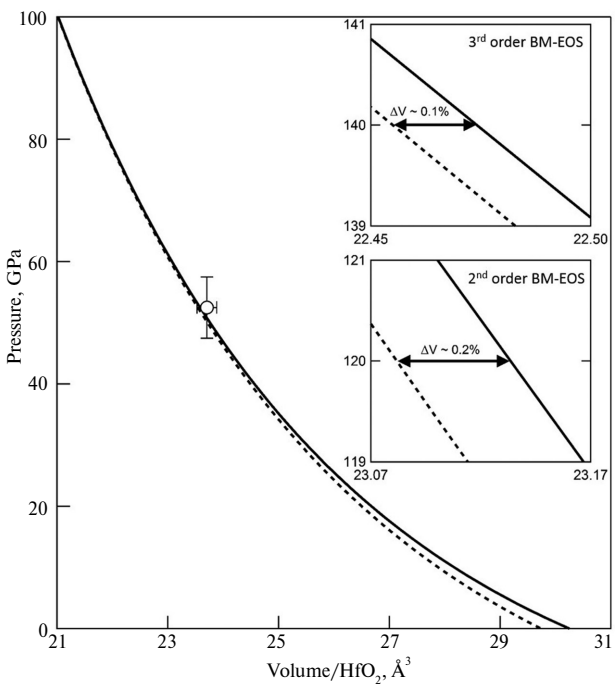

Fig. 5. Pressure versus volume of one HfO_2 formula unit as determined by GGA computations using the third-order BM-EOS [52]. The solid line represents the OII phase, whereas the dashed line represents the Fe_2P phase. The open circle represents the measured volume of Fe_2P–HfO_2 at ~ 105 GPa [9], which agrees well with the calculated volume at the same pressure. Our calculations clearly show the small volume change between the two phases especially at high pressures. The volume collapse at the transition pressure between the two phases is shown in the insets (upper inset: using the third-order BM-EOS, lower inset: using the second-order BM-EOS).

Table 3. The expected versus measured *d*-spacing values for the three observed weak XRD reflections at 105 GPa [9] and the corresponding measured volume for one HfO_2 formula unit and the unit-cell parameters

hkl	Expected *d*-spacing, Å	Measured *d*-spacing, Å	Difference between expected and measured values, Å
201	1.8088	1.8173	–0.0085
101	2.5178	2.5146	+0.0032
110	2.6003	2.5974	+0.0029
Volume, $Å^3$	23.71 (0.18)		
Unit-cell parameters, Å	a = 5.2005 (0.0182), c = 3.0366 (0.0170)		

Volume change

As shown in Fig. 5, the OII → Fe_2P transition in HfO_2 is associated with a slight volume change of ~ 0.2 % (0.1 %) using the second- (third-) order BM-EOS [52] at the transition pressure. In fact, this result is not unexpected since the coordination number (CN) of Hf in Fe_2P phase remains unchanged upon the transition from OII phase, where the CN of Hf is 9 in both phases. However, this volume difference increases as pressure decreases, and it reaches ~ 1.2 % (1.7 %) using the second- (third-) order BM-EOS [52] at zero pressure (see Fig. 5, Table 1) indicating that Fe_2P is the densest known phase of HfO_2 in good agreement with recent GGA calculations where Fe_2P phase is found to be 1.9 % and 1.0 % denser than OII phase (Table 1) for TiO_2 [39] and ZrO_2 [40], respectively. Furthermore, the slight volume drop across OII → Fe_2P transition has been also observed in recent measurements for both TiO_2 [39] and ZrO_2 [40] and it has been concluded that Fe_2P is the densest phase at these conditions among TiO_2 and ZrO_2 polymorphs as well, consistent with our predictions.

Generally, we note that if the transition from one phase to another is associated with an increase in the CN of the central atom, a large volume change is expected, which is not the case for the OII → Fe_2P transition. For instance, the OI → OII transition in HfO_2 corresponds to an increase of the CN in Hf from 7 to 9, and, therefore, a large volume collapse has been reported both experimentally [9, 11, 26] and theoretically [9, 22, 25].

Hardness calculations

For completeness, we introduce a brief discussion on the mechanical hardness of TMDs to support our prediction of the post-cotunnite phase. Over the last two decades, high-pressure phases of TMDs have been suggested to possess high hardness values (for a recent review, see Ref. [58]). However, recent studies have concluded that none of these phases are qualified to be superhard in spite of their high bulk moduli [9, 27, 58–60]. To test this conclusion, we use the Simunek and Vackar scaling model [53] to estimate the hardness of Fe_2P–HfO_2 at equilibrium and compare it with that of the other crystal structures of HfO_2. In this model, the hardness is inversely proportional to average atomic volume, coordination number, and bond length, whereas it is proportional to the average number of bonds per atom [53]. Based on this model, the hardness is also dependent on the characteristic length scale of the charge density distribution about each atom (R_i), where R_i is found to be nearly independent of phase [9, 27, 53, 61] with values of 1.78 Å and 1.07 Å for Hf and O, respectively, using GGA calculations [9].

As expected, since Fe_2P–HfO_2 is slightly denser than OII–HfO_2, our computed Hf–O bond lengths in Fe_2P–HfO_2 are found to be slightly shorter in OII–HfO_2, where both phases have the same CN; thus, a slight increase in hardness is expected for Fe_2P compared to OII. Indeed, our calculated hardness for OII is 9.8 GPa in excellent agreement with previous calculations [9], whereas our calculated value for Fe_2P is 10 GPa which is only ~2 % higher than that of OII. Furthermore, the fact that Fe_2P does not qualify to be potentially superhard has been also confirmed for TiO_2 with a computed hardness value of less than 20 GPa [59]. Therefore, our hardness calculations confirm that high-pressure phases of TMDs do not qualify to be superhard materials as their hardness is much less than 40 GPa, a prerequisite for a material to be superhard. We emphasize that while Fe_2P–HfO_2 is not superhard, it may show other interesting properties; however, the focus of this study is on the confirmation of this phase at extreme *p*, *T*-conditions, similar to other TMDs.

CONCLUSIONS

In summary, we have tested the stability of a new post-cotunnite phase at high pressures using DFT-based *first-principles* computations, and concluded that Fe_2P is the highest pressure and the densest phase of HfO_2 determined thus far. Our prediction of the new phase is consistent with previous measurements and calculations performed on similar TMDs TiO_2 [39] and ZrO_2 [40] in terms of the EOS, transition pressure, and volume change as well as the trends in these outcomes among the three TMDs. Importantly, our re-analysis of previous DAC-XRD measurements on HfO_2 at extreme conditions (105 GPa, 1800 K) [9] has shown that the experimental OII $\rightarrow$ Fe_2P transition pressure is likely to be close to our calculated value (~ 120–140 GPa) in agreement with the expected experimental transition pressure when compared to the measured values in TiO_2 [39] and ZrO_2 [40]. Additionally, our mechanical hardness estimations of the dense Fe_2P–HfO_2 phase clearly show that the newly predicted phase is not a candidate for a superhard material.

ACKNOWLEDGMENTS

This work was completed utilizing the Holland Computing Center of the University of Nebraska.

Використовуючи розрахунки з перших принципів теорії функціонала щільності, спрогнозовано отримання за високого тиску нової фази пост-хлориду свинцю (OII) – двоокису гафнію (HfO_2). Наші розрахунки, з використанням наближення узагальненого градієнта, передбачають фазовий перехід від OII до структури типу Fe_2P при ~ 120 ГПа (~ 140 ГПа) з невеликою зміною об'єму з перепадом тиску ~ 0,2 % (~ 0,1 %) між двома фазами з використанням другого (третього) порядку рівняння Birch-Murnaghan. Прогнозування нової фази узгоджується з останніми експериментами та розрахунками, проведеними на подібних діоксидах титану (TiO_2) та цирконію (ZrO_2) при екстремальних температурних умовах. Важливо, що наш теоретичний прогноз для переходу OII $\rightarrow$ Fe_2P в HfO_2 експериментально підтверджується повторним аналізом рентгеноструктурних картин HfO_2 за екстремальних тиску та температури. Крім того, було розраховано рівняння стану і твердість передбачуваної фази та показано, що фаза типу Fe_2P, хоча мала меншу стисливість, ніж фаза OII, є практично ідентичною з останньою за твердістю, і це вказує, що жодна з фаз HfO_2 не є надтвердою.

***Ключові слова**: фазові переходи, рівняння стану, твердість, первинні принципи, рентгенівська дифракция, фазова стабільність.*

Используя вычисления из первых принципов теории функционала плотности, предсказано получение при высоких давлениях новой фазы пост-хлорида свинца

(OII) – двуокиси гафния (HfO_2). Наши расчеты, используя приближение обобщенного градиента, предсказывают фазовый переход от OII к структуре типа Fe_2P при ~ 120 ГПа (~ 140 ГПа) при небольшом изменении объема при давлении перехода ~ 0,2 % (~ 0,1 %) между двумя фазами с использованием уравнения состояния второго (третьего) порядка Birch-Murnaghan. Предсказание новой фазы согласуется с недавними экспериментами и расчетами, выполненными на аналогичных диоксидах титана (TiO_2) и циркония (ZrO_2) в экстремальных температурных условиях. Важно отметить, что наше теоретическое предсказание для перехода OII $\rightarrow Fe_2P$ в HfO_2 экспериментально подтверждается повторным анализом рентгеновских дифрактограмм HfO_2 при экстремальных давлении и температуре. Кроме того, было вычислено уравнение состояния и твердость предсказанной фазы и показано, что фаза типа Fe_2P, хотя имела меньшую сжимаемость, чем фаза OII, почти идентична с последнею по твердости, этоуказывает на то, что ни одна из фаз HfO_2 не является сверхтвердой.

***Ключевые слова**: фазовые переходы, уравнение состояния, твердость, первые принципы, рентгеновская дифракция, фазовая устойчивость.*

1. *Khoshman J. M., Khan A., Kordesch M. E.* Amorphous hafnium oxide thin films for antireflection optical coatings // Surf. Coatings Technol. – 2008. – **202**. – P. 2500–2502.
2. *Torchio P., Gatto A., Alvisi M., Albrand G., Kaiser N., Amra C.* High-reflectivity HfO_2/SiO_2 ultraviolet mirrors // Appl. Opt. – 2002. – 41. – P. 256–3261.
3. Choi J. H., Mao Y., Chang J. P. Development of hafnium based high-k materials - A review // Mater. Sci. Eng. R Reports. – 2011. – **72**. – P. 97–136.
4. *Zhu H., Tang C., Fonseca L. R. C., Ramprasad R*. Recent progress in ab initio simulations of hafnia-based gate stacks // J. Mater. Sci. – 2012. – **47**. – P. 7399–7416.
5. *Robertson J., Wallace R. M.* High-K materials and metal gates for CMOS applications // Mater. Sci. Eng. R Reports. – 2015. – **88**. – P. 1–41.
6. *Bersuker G., Gilmer D. C., Veksler D., Kirsch P., Vandelli L., Padovani A., Larcher L., McKenna K., Shluger A., Iglesias V., Porti M., Nafria M.* Metal oxide resistive memory switching mechanism based on conductive filament properties // J. Appl. Phys. 2011. – **110**, N 12, art. 124518.
7. P*rivitera S., Bersuker G., Butcher B., Kalantarian A., Lombardo S., Bongiorno C., Geer R., Gilmer D. C., Kirsch P. D.* Microscopy study of the conductive filament in HfO_2 resistive switching memory devices // Microelectron. Eng. – 2013. – **109**. – P. 75–78.
8. *Lin K. L., Hou T. H., Shieh J., Lin J.-H., Chou Ch.-T., Lee Y.-J.* Electrode dependence of filament formation in HfO_2 resistive-switching memory // J. Appl. Phys. – 2011. – **109**, art. 084104.
9. *Al-Khatatbeh Y., Lee K. K. M, Kiefer B*. Phase diagram up to 105 GPa and mechanical strength of HfO_2. Phys. Rev. B. – 2010. – **82**, art. 144106.
10. *Haines J., Leger J. M., Hull S., Petitet J. P., Pereira A. S., Perottoni C. A., da Jornada J. A. H.* Characterization of the cotunnite-type phases of zirconia and hafnia by neutron diffraction and Raman spectroscopy // J. Am. Ceram. Soc. – 1997. – **80**. – P. 1910–1914.
11. *Desgreniers S., Lagarec K.* High-density ZrO_2 and HfO_2: Crystalline structures and equation of state // Phys. Rev. B. – 1999. – 59. – P. 8467–8472.
12. *Adams D. M., Leonard S., Russell D. R., Cernik R. J.* X-ray diffraction study of hafnia under high pressure using synchrotron radiation // J. Phys. Chem. Solids. – 1991. – **52**. – P. 1181–1186.
13. *Leger J. M., Haines J, Blanzat B.* Materials potentially harder than diamond: Quenchable high-pressure phases of transition metal dioxides // J. Mater. Sci. Lett. – 1994. – 13. – P. 1688–1690.
14. *Jayaraman A.* Diamond anvil cell and high-pressure physical investigations // Rev. Mod. Phys. – 1983. – **55**. – P. 65–108.
15. *Ohtaka O., Yamanaka T., Kume S., Izumi F.* Synthesis and X-ray structural analysis by the Rietveld method of orthorhombic hafnia // J. Ceram. Soc. Japan. – 1991. – **99**. – P. 826–827.
16. *Ohtaka O., Yamanaka T., Kume S., Hara N., Asano H., Izumi F.* Structural analysis of orthorhombic hafnia by neutron powder diffraction // J. Am. Ceram. Soc. – 1995. – **78**. – P. 233–237.
17. *Arashi H., Yagi T., Akimoto S., et al.* New high-pressure phase of ZrO_2 above 35 GPa // Phys. Rev. B. – 1990. – **41**. – P. 4309–4313.

18. *Leger J. M., Atouf A., Tomaszewski P. E., Pereira A. S.* Pressure-induced phase transtions and volume changes in HfO_2 up to 50 GPa // Phys. Rev. B. – 1993. – **48**. – P. 93–98.
19. *Mandal G., Jana R., Saha P., Das P.* Study of structural phase transition of HfO_2 at high pressure // Mater. Today Proc. – 2016. – **3**. – P. 2997–3001.
20. *Mandal G., Das P.* The pressure induced structural phase transition of HfO_2 // AIP Conf. Proc. – 2017, art. 30014.
21. *Terki R., Bertrand G., Aourag H., Coddet C.* Cubic-totetragonal phase transition in HfO_2 from computational study // Mater. Lett. – 2008. – **62**. – P. 1484–1486.
22. *Jaffe J. E., Bachorz R. A., Gutowski M.* Low-temperature polymorphs of ZrO_2 and HfO_2: A density-functional theory study // Phys. Rev. B. – 2005. – **72**, art. 144107.
23. *Lowther J. E., Dewhurst J. K., Leger J. M., Haines J.* Relative stability of ZrO_2 and HfO_2 structural phases // Phys. Rev. B. – 1999. – **60**. – P. 14485–14488.
24. *Dewhurst J. K., Lowther J. E.* Highly coordinated metal dioxides in the cotunnite structure // Phys. Rev. B. – 2001. – **64**, art. 14104.
25. *Kang J., Lee E.-C., Chang K. J.* First-principles study of structural phase transformation of hafnia under pressure // Phys. Rev. B. – 2003. – **68**, art. 54106.
26. *Ohtaka O., Fukui H., Kunisada T., Fujisawa T.* Phase relations and volume changes of hafnia under high pressure and high temperature // J. Am. Ceram. Soc. – 2001. – **84**. – P. 1369–1373.
27. *Al-Khatatbeh Y., Lee K. K. M, Kiefer B.* Phase relations and hardness trends of ZrO2 phases at high pressure // Phys. Rev. B. – 2010. – **81**, art. 214102.
28. *Ohtaka O., Andrault D., Bouvier P., Schultz E., Mezouar M.* Phase relations and equation of state of ZrO_2 to 100 GPa // J. Appl. Crystallogr. – 2005. – **38**. – P. 727–733.
29. *Ohtaka O., Fukui H., Funakoshi K., Utsumi W., Irifune T., Kikegawa T.* Phase relations and EOS of ZrO_2 and HfO2 under high-temperature and high-pressure // High Press. Res. – 2002. – **22**. – P. 221–226.
30. *Ohtaka O., Fukui H., Kunisada T., Fujisawa T., Funakoshi K., Utsumi W., Irifune T., Kuroda K., Kikegawa T.* Phase relations and equations of state of ZrO_2 under high temperature and high pressure // Phys. Rev. B. – 2001. – **63**, art. 174108.
31. *Fadda G., Colombo L., Zanzotto G.* First-principles study of the structural and elastic properties of zirconia // Phys. Rev. B. – 2009. – **79**, art. 214102.
32. *Al-Khatatbeh Y., Lee K. K. M., Kiefer B.* High-pressure behavior of TiO_2 as determined by experiment and theory // Phys. Rev. B. – 2009. – **79**, art. 134114.
33. *Dubrovinskaia N. A., Dubrovinsky L. S., Ahuja R., Prokopenko V. B., Dmitriev V., Weber H. P.* Experimental and theoritical identification of a new high-pressure TiO_2 polymorph // Phys. Rev. Lett. – 2001. – **87**, art. 275501.
34. *Dubrovinsky L. S., Dubrovinskaia N. A., Swamy V., Muscat J., Harrison N. M., Ahuja R., Holm B., Johansson B.* The hardest known oxide // Nature. – 2001. – **410**. – P. 653–654.
35. *Nishio-Hamane D., Shimizu A., Nakahira R. et al.* The stability and equation of state for the cotunnite phase of TiO_2 up to 70 GPa // Phys. Chem. Miner. – 2009. – **37**. – P. 129–136.
36. *Mattesini M., de Almeida J. S., Dubrovinsky L., Dubrovinskaia N., Johansson B., Ahuja R.* High-pressure and high-temperature synthesis of the cubic TiO_2 polymorph // Phys. Rev. B. – 2004. – **70**, art. 212101.
37. *Caravaca M. A., Mino J. C., Pérez V. J., Casali R A., Ponce C. A.* Ab initio study of the elastic properties of single and polycrystal TiO_2, ZrO_2 and HfO_2 in the cotunnite structure // J. Phys. Condens. Matter. – 2009. – **21**, art. 15501.
38. *Muscat J., Swamy V., Harrison N. M.* First-principles calculations of the phase stability of TiO_2 // Phys. Rev. B. – 2002. – **65**, art. 224112.
39. *Dekura H., Tsuchiya T., Kuwayama Y., Tsuchiya J.* Theoretical and experimental evidence for a new post-cotunnite phase of titanium dioxide with significant optical absorption // Phys. Rev. Lett. – 2011. – **107**, art. 45701.
40. *Nishio-Hamane D., Dekura H., Seto Y., Yagi T.* Theoretical and experimental evidence for the post-cotunnite phase transition in zirconia at high pressure // Phys. Chem. Miner. – 2015. – 42. – P. 385–392.
41. *Meng X., Wang L., Liu D., Wen **X**., Zhu Q., Goddad W. A., An Q.* Discovery of Fe_2P-type $Ti(Zr/Hf)_2O_6$ photocatalysts toward water splitting // Chem. Mater. – 2016. – **28**. – 1335–1342.
42. *Hohenberg P., Kohn W.* Inhomogeneous electron gas // Phys. Rev. – 1964. – **136**. – P. B864–B871.
43. *Kresse G., Joubert D.* From ultrasoft pseudopotentials to the projector augmented-wave method // Phys. Rev. B. – 1999. – **59**. – P. 1758–1775.

44. *Blochl P. E.* Projector augmented-wave method // Phys. Rev. B. – 1994. – **50**, art. 17953.
45. *Perdew J. P., Burke K., Ernzerhof M.* Generalized gradient approximation made simple // Phys. Rev. Lett. – 1996. – **77**. – P. 3865–3868.
46. *Kresse G., Furthmuller J.* Efficiency of ab-initio total energy calculations for metals and semiconductors using a plane-wave basis set // Comput. Mater. Sci. – 1996. – **6**. – P. 15–50.
47. *Kresse G., Furthmuller J.* Efficient iterative schemes for ab initio total-energy calculations using a plane-wave basis set // Phys. Rev. B. – 1996. – **54**. – P. 11169–11186.
48. *Kresse G., Hafner J.* Norm-conserving and ultrasoft pseudopotentials for first-row and transition elements // J. Phys. Condens. Matter. – 1994. – **6**, art. 8245.
49. *Kresse G., Hafner J.* Ab initio molecular dynamics for open-shell transition metals // Phys. Rev. B. – 1993. – **48**. – P. 13115–13118.
50. *Monkhorst H. J., Pack J. D.* Special points for Brillouin-zone integrations // Phys. Rev. B. – 1976. – **13**. – P. 5188–5192.
51. *Wang L.-L., Johnson D. D.* Removing critical errors for DFT applications to transition-metal nanoclusters: Correct ground-state structures of Ru clusters // J. Phys. Chem. B. 2005. – **109**. – P. 23113–23117.
52. *Birch F.* Elasticity and constitution of the Earth's interior // J. Geophys. Res. – 1952. – **57**. – P. 227–234.
53. *Simunek A., Vackar J.* Hardness of covalent and ionic crystals: First-principle calculations // Phys. Rev. Lett. – 2006. – **96**, art. 85501.
54. *Wang Y., Panzik J. E., Kiefer B., et al.* Crystal structure of graphite under room-temperature compression and decompression // Sci. Rep. – 2012. – **2**, art. 520.
55. *Heinz D. L.* Thermal pressure in the laser-heated diamond anvil cell // Geophys. Res. Lett. – 1990. – **17**. – P. 1161–1164.
56. *Goncharov A. F., Prakapenka V. B., Struzhkin V. V., Kantor I., Rivers M. L., Dalton D. A.* X-ray diffraction in the pulsed laser heated diamond anvil cell // Rev. Sci. Instrum. – 2010. – **81**, art. 113902.
57. *Andrault D., Fiquet G., Itie J. P., Pascal R., Philippe G., Häusermann D., Hanfland M.* Thermal pressure in the laser-heated diamond-anvil cell: An X-ray diffraction study // Eur. J. Mineral. – 1998. – **10**. – P. 931–940.
58. *Al-Khatatbeh Y., Lee K. K. M.* From superhard to hard: A review of transition metal dioxides TiO_2, ZrO_2, and HfO_2 hardness // J. Superhard Mater. – 2014. – **36**. – P. 231–245.
59. D*ing Y., Chen M., Wu W.* Mechanical properties, hardness and electronic structures of new post-cotunnite phase (Fe_2P-type) of TiO_2 // Phys. B: Condens. Matter. – 2014. – **433**. – P. 48–54.
60. *Lyakhov A. O., Oganov A. R. E*volutionary search for superhard materials: Methodology and applications to forms of carbon and TiO_2 // Phys. Rev. B. – 2011. – **84**, art. 92103.
61. *Simunek A.* How to estimate hardness of crystals on a pocket calculator // Phys. Rev. B. – 2007. – **75**, art. 172108.
62. *Momma K., Izumi F.* VESTA 3 for three-dimensional visualization of crystal, volumetric and morphology data // J. Appl. Crystallogr. – 2011. – **44**. – P. 1272–1276.
63. *Haines J., Leger J. M., Atouf A.* Crystal structure and equation of state of cotunnite-type zirconia // J. Am. Ceram. Soc. – 1995. – **78**. – P. 445–448.

Received 19.03.18
Revised 15.04.18
Accepted 15.04.18